

See discussions, stats, and author profiles for this publication at: <https://www.researchgate.net/publication/259311487>

Physical Aging of Polymer Films Quenched and Measured Free-Standing via Ellipsometry: Controlling Stress Imparted by Thermal Expansion Mismatch between Film and Support

ARTICLE *in* MACROMOLECULES · NOVEMBER 2013

Impact Factor: 5.8 · DOI: 10.1021/ma401872u

CITATIONS

13

READS

39

2 AUTHORS, INCLUDING:



Justin Edward Pye

Emory University

6 PUBLICATIONS 125 CITATIONS

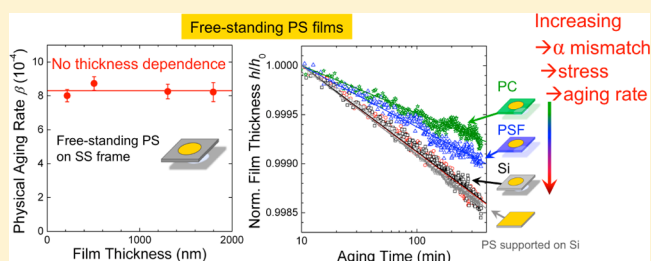
SEE PROFILE

Physical Aging of Polymer Films Quenched and Measured Free-Standing via Ellipsometry: Controlling Stress Imparted by Thermal Expansion Mismatch between Film and Support

Justin E. Pye and Connie B. Roth*

Department of Physics, Emory University, Atlanta, Georgia 30322, United States

ABSTRACT: We have developed an ellipsometry method to measure the physical aging rate of polymer films that have been thermally quenched and aged in a free-standing state where the stress imparted to the films is well-defined by the thermal-expansion mismatch between film and rigid support. For free-standing polystyrene films supported by rigid sample holders with circular openings, we demonstrate that the physical aging rate is independent of film thickness between 220 and 1800 nm when the applied stress is the same. In contrast, by comparing free-standing films supported by frames of different materials, the physical aging rate decreases by nearly a factor of 2 when the thermal-expansion mismatch, and hence stress, is reduced. We conclude that stress is key in controlling the resulting physical aging rate of free-standing films, and there is no inherent film-thickness dependence (above 220 nm) to the aging rate when stress during glass formation is held fixed.



INTRODUCTION

The nonequilibrium nature of glasses results in materials whose mechanical, electrical, and optical properties evolve with time as the system slowly relaxes toward equilibrium, a process referred to as structural relaxation or physical aging. Understanding how physical aging of polymer glasses is affected by thermal and processing histories in thin films is crucial for applications ranging from gas separation membranes to barrier and dielectric layers.^{1,2} During the past 18 years, a number of studies have reported “accelerated” or faster physical aging of free-standing polymer films with decreasing thickness.^{3–10} These deviations from bulk properties have been observed at surprisingly large length scales when films are still hundreds to thousands of nanometers in thickness. This is in contrast to changes in physical aging observed in films less than ~ 100 nm in thickness^{11–18} that have been linked to changes in the glass transition temperature (T_g).^{19,20} Previous studies have interpreted the cause of the accelerated aging at the longer length scales as some inherent film thickness dependence associated with glassy dynamics by fitting the data to a free volume diffusion model with lattice contraction.^{5,10,21–24} More recently, Gray et al. proposed an alternative explanation suggesting that the accelerated aging may result from increased stress imparted to the films by their mechanical support.⁸ Here, we present results that demonstrate there is no inherent film thickness dependence (above 220 nm) to the aging rate of free-standing polystyrene (PS) films when held by rigid frames that impart a thickness-independent stress on cooling.

Accelerated physical aging of thin polymer films was first characterized by gas permeation measurements.^{3–7} As a function of aging time, the gas permeability of the films, which is extremely sensitive to free volume in the membranes,

was found to decrease more rapidly for thinner films. Although it is not straightforward to determine a physical aging rate from permeability data,²³ McCaig and Paul^{5,21} interpreted their results in terms of a free volume diffusion and lattice contraction model originally developed by Curro et al.²⁵ This model proposes a microscopic interpretation for volume recovery that treats vacancy propagation as an effective diffusion of local free volume. The only adjustable parameter is a somewhat arbitrary diffusion length scale that defines the characteristic relaxation time.²⁵ To avoid a dependence of T_g and physical aging rate on the macroscopic size of the sample, Curro et al. suggested that some “internal length scale” might exist over which free volume can be created or annihilated. To date, the existence of such “internal interfaces” has not yet been definitively determined.¹⁰ Following an idea originally proposed by Alfrey et al.²⁶ where free volume “holes” that diffuse to the surface of a sample would disappear, McCaig and Paul^{5,21} related the diffusion length scale to the macroscopic thickness of their free-standing films. Such a model was found to fit the data remarkably well and has since been adapted by others to explain accelerated aging behavior observed in thin films by positron annihilation lifetime spectroscopy (PALS),^{22,24,27} differential scanning calorimetry,¹⁰ dielectric spectroscopy,²⁴ ellipsometry and gas permeation.^{22,23,28} Similar ideas have also been applied to accelerated aging observed in polymer nanocomposites where possible voids at the nanofiller interface are assumed to contribute to the internal interfaces at which free volume can be annihilated.^{29,30} In many of these studies,

Received: September 9, 2013

Revised: November 11, 2013

Published: November 20, 2013

this internal length scale is treated as a fitting parameter with values typically being several micrometers in size.^{10,22,24,29,30} Recently, Rowe et al.²⁷ have used variable energy PALS to measure the local free volume as a function of depth near the free surface. Although the size of the free volume "holes" were found to be reduced near the free surface, the size and number of holes maintained a constant depth profile with aging time, in contrast to what would be anticipated based on the free volume diffusion model.²¹ Overall, these studies argue the key to accelerated aging is the presence of free surface or internal interface at which free volume can be annihilated or created, implying an inherent film thickness dependence to physical aging.

More recently, an alternative explanation has been proposed to account for the accelerated physical aging behavior observed in micrometer thick films. Gray et al.⁸ observed that the thickness-dependent accelerated aging was only present for films that were quenched free-standing on thin wire frames, mimicking the sample preparation of the gas permeation studies.⁷ It was proposed that these wire frames (made of 0.009 in. diameter spring steel) flexed, acting as small springs imparting a stress, σ = force/area, to the samples that depended on the cross-sectional area of the films (film thickness \times width), such that the stress increased with decreasing film thickness.⁸ This is in contrast to free-standing films supported by inflexible rigid frames which impart a thickness-independent stress to the films on cooling that depends on the thermal expansion mismatch between the polymer films and rigid frame (as calculated below). Such stresses on free-standing films supported by rigid frames caused by thermal expansion mismatch are equivalent to the well-documented and experimentally measured^{31–33} stresses experienced by supported polymer films on rigid substrates (e.g., silicon). For PS on silicon the difference in thermal expansion coefficients is roughly 2 orders of magnitude resulting in stress values of ~ 15 MPa when cooled to room temperature, consistent with experimental measurements.^{31,32} The idea of stress during the thermal quench affecting the subsequent aging of the glass is supported by work on *o*-terphenyl confined to nanoporous glasses,³⁴ polymer nanospheres,³⁵ and from observations that the aging rate is independent of film thickness for supported films above ~ 100 nm in thickness.^{8,11}

Here, we present results strongly suggesting that unintended stresses during thermal cooling from differences in thermal expansion between film and support can strongly affect the subsequent physical aging behavior of micrometer thick free-standing glassy films. To accomplish this, we have developed a method of measuring the volumetric physical aging rate of polymer films that have been quenched and remain free-standing during the aging process. To our knowledge, this is the first report of in-situ physical aging measurements by ellipsometry on films that remain in their free-standing state during the aging process. Free-standing films held by rigid frames are used to impart a well-defined and film-thickness-independent stress to the films during the thermal quench. The time-dependent decrease in thickness and increase in index of refraction resulting from the densification of the films as a function of aging time were measured by transmission ellipsometry. For films between 220 and 1800 nm in thickness, we observe no change in physical aging rate as a function of film thickness for films held by stainless steel (SS) frames with a circular opening. This is consistent with the thickness-independent in-plane stress of $\sigma \approx 4.5$ MPa imparted to the

films during the thermal quench to an aging temperature of 65 °C, caused by thermal expansion mismatch between PS and the SS frame. We establish that this stress affects the physical aging rate and verify its source by demonstrating that the aging rate of PS correlates with the stress caused by thermal-expansion mismatch between film and rigid support for a series of different frame materials: silicon (Si), stainless steel (SS), aluminum (Al), polysulfone (PSF), and polycarbonate (PC).

EXPERIMENTAL SECTION

Films were made by spin-coating PS (M_w = 3240 kg/mol, M_w/M_n = 1.05, Polymer Laboratories) dissolved in toluene onto silicon or freshly cleaved mica. Film thickness was controlled by adjusting the spin speed and solution concentration. Films were typically spun at speeds between 600 and 1000 rpm; no effect of spin speed on aging was observed even for films spun at 4000 rpm. All films were annealed for at least 12 h at 130 °C under vacuum to remove residual solvent and relax stresses induced during spin-coating and then cooled slowly on mica at <0.5 °C/min through T_g . Free-standing films were produced by floating onto Si ($\langle 100 \rangle$ orientation), 304 stainless steel (SS), 6061 aluminum (Al), polysulfone (PSF) (Tecason S), or polycarbonate (PC) (RowTec) frames with a 5 mm diameter circular opening. To initiate the aging measurements, PS films were rejuvenated for 20 min at 120 °C before quenching to room temperature at 90 °C/min in the free-standing state using an Instec hot stage with liquid nitrogen cooling. The Instec hot stage has a small interior chamber (50 mm in length \times 38 mm in width \times 2 mm in height), giving only 3.8 cm³ volume of air surrounding the free-standing film that needs to be heated or cooled. As discussed in Gray et al.,⁸ heat transfer to thin free-standing films from the surrounding air is very efficient. The free-standing film is oriented horizontally in the chamber with the cover containing a window such that the film can be viewed during the annealing step. Shortly after heating above T_g , surface tension acts to smooth out wrinkles after which the film remains flat. Rapid cooling of the film is achieved by pumping liquid nitrogen through the heater base. Using an external thermocouple mounted to the sample, we have measured this to be 90 °C/min. Immediately after quenching, films were transferred to another heater that had been equilibrated at the aging temperature for at least 30 min. The time from the beginning of the quench to the start of the aging measurement was kept as short as possible (~ 4 min). Measurements were performed with a J.A. Woollam M-2000 ellipsometer in transmission and reflection geometry for free-standing and supported films, respectively. Free-standing films were held at an angle of 45° with respect to the beam and modeled by a single Cauchy layer with $n(\lambda) = A + B/\lambda^2 + C/\lambda^4$ for λ from 400 to 1000 nm.²⁰ Supported films were measured at 65° angle of incidence and modeled as a Cauchy layer on top of a silicon substrate (with temperature-dependent optical properties)¹¹ and a 2 nm native oxide layer.¹¹

RESULTS AND DISCUSSION

Physical Aging of Films Quenched and Measured Free-Standing via Ellipsometry. Previous efforts in our lab to test the impact of stress imparted to films during the thermal quench caused by differences in thermal expansion mismatch were hampered by excessive wrinkling and buckling of the free-standing films limiting reproducibility.⁸ For the present study, we have made three key improvements to our experimental procedure that prevent wrinkling of the films: smaller samples sizes (5 mm diameter instead of 19 mm), a more controlled quench environment that minimizes air currents and has a controlled quench rate of 90 °C/min, and measurement of the aging rate in the free-standing state via transmission ellipsometry such that the films do not need to be transferred to silicon substrates for the subsequent aging. These changes enable the measurement of reproducible physical aging rates for

free-standing films quenched on rigid frames where the stress imparted by thermal expansion mismatch between the film and frame can be explicitly calculated.

Figure 1 plots the normalized film thickness (h/h_0) as a function of logarithmic aging time for several 515 ± 10 nm

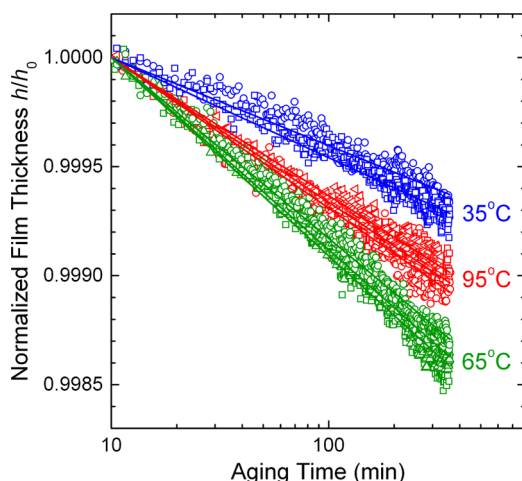


Figure 1. Normalized film thickness h/h_0 vs logarithmic aging time for 515 ± 10 nm thick free-standing films on stainless steel (SS) frames aged at 35, 65, and 95 °C. Several aging measurements and fit lines are shown for each aging temperature demonstrating the excellent reproducibility of the measurement.

thick free-standing PS films draped across SS frames with a circular opening aged at different temperatures. We quantify the physical aging rate by calculating the slope of the data plotted in this manner: $\beta = -\partial(h/h_0)/\partial(\log t)$, where h_0 is the film thickness at an aging time of 10 min and t is the aging time.^{8,11,36} Defined in this way, β is equivalent to a volumetric aging rate,³⁶ as originally established by Struik.³⁷ Figure 1 shows data collected at three different aging temperatures with several aging measurements shown for each temperature demonstrating reproducibility: $\beta = (4.3 \pm 0.4) \times 10^{-4}$ at 35 °C, $(8.7 \pm 0.4) \times 10^{-4}$ at 65 °C, and $(6.6 \pm 0.3) \times 10^{-4}$ at 95 °C. The errors are calculated based on the standard deviation of 2–3 measurements at each aging temperature on nominally identical samples. We note the data shown in Figure 1 are for aging times up to 6 h, but measurements were also done for aging times up to 24 h with no deviation observed in the linear decrease in film thickness with logarithmic aging time, giving identical aging rates for longer runs when the aging temperature was 65 °C and above, while at 35 °C the aging rates of the shorter runs only deviated by 6% relative to the longer runs. For experimental efficiency, aging runs were typically limited to 6 h.

The temperature dependence of the physical aging rate for 515 ± 10 nm thick free-standing PS films on SS frames is plotted in Figure 2. For comparison, the temperature dependence of supported PS films of equivalent thickness (490 ± 10 nm) on silicon are also graphed. The supported data are consistent with our previous measurements on supported PS films^{11,36} but have been retaken to match the quench rate of the free-standing films in this study (90 °C/min), as differences in cooling rate can affect the measured aging rate.⁸ The physical aging rates of both free-standing and supported films exhibit a qualitatively similar temperature dependence with a peak near 65 °C. The small quantitative difference in aging rates can be

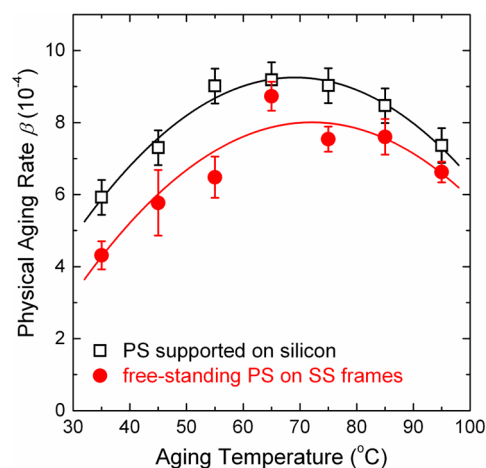


Figure 2. Temperature dependence of physical aging rate β for ~ 500 nm thick PS films held free-standing on stainless steel frames (solid red circles) and supported on silicon (open black squares). Error bars for free-standing films are the standard deviations of several measurements. For the supported films, several measurements were taken at 65 °C to determine a representative error bar for all temperatures.

explained by the small difference in stress applied to the films, as described below. The peak in aging rate occurs because as the temperature is decreased below T_g , the driving force for structural relaxation increases with decreasing temperature until, at sufficiently low temperatures, the reduced thermal energy available limits any significant motion of the local structural units.

Focusing on the peak in aging rate at 65 °C, measurements as a function of film thickness were carried out on free-standing films held by the SS frames. Figure 3 shows that for free-standing films with thicknesses between 220 and 1800 nm, the measured physical aging rates are all within experimental error of each other: $\beta_{220 \text{ nm}} = (8.0 \pm 0.4) \times 10^{-4}$, $\beta_{500 \text{ nm}} = (8.7 \pm 0.4) \times 10^{-4}$, $\beta_{1330 \text{ nm}} = (8.3 \pm 0.4) \times 10^{-4}$, and $\beta_{1800 \text{ nm}} = (8.2 \pm 0.6) \times 10^{-4}$. These results are in contradiction with predictions by the free volume diffusion model previously used to explain

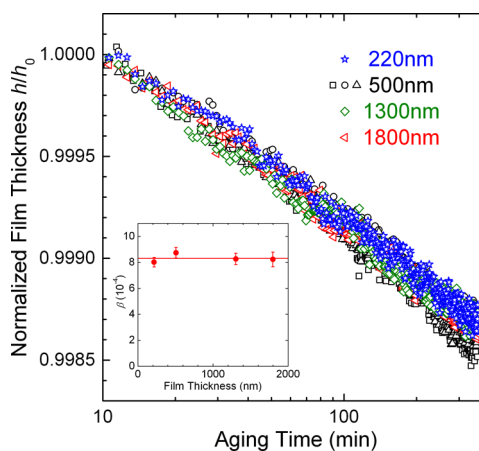


Figure 3. Normalized film thickness h/h_0 vs logarithmic aging time for free-standing PS films held by SS frames and aged at 65 °C. Data for varying thicknesses from 220 to 1800 nm are plotted, with several measurements of 500 nm thick films shown for comparison indicating sample-to-sample variability. Inset: average physical aging rate β as a function of film thickness.

faster aging rates with decreasing thickness observed in free-standing films.^{5,10,21–24} However, as discussed in the following section, these results are in agreement with a constant, film-thickness-independent stress occurring from the thermal expansion mismatch between film and support.

Thermal Stresses Imparted to Free-Standing Films by Rigid Frames on Cooling. For a thin polymer film cooled on a rigid support, the in-plane strain of the polymer film is constrained to match that of the rigid support. For the case of PS supported on silicon, the difference in thermal expansion between film and substrate is roughly 2 orders of magnitude. Thus, during a thermal cool, the PS film will try to thermally contract more than the underlying silicon. Forcing the PS strain to match that of the silicon substrate imparts an equibiaxial in-plane stress onto the PS film. The magnitude of this stress can be readily determined from standard stress–strain considerations.

Starting from the general elastic stress–strain relationships for a triaxial stress with thermal strain,³⁸ for an equibiaxial strain ($\epsilon_x = \epsilon_y$) under plane-stress conditions we set $\sigma_x = \sigma_y = \sigma$ and $\sigma_z = 0$ because there is no stress normal to the film plane as the film is unconstrained in this direction. The in-plane (ϵ_x) and out-of-plane (ϵ_z) strains are written as

$$\epsilon_x = \frac{\sigma}{E_{\text{PS}}}(1 - \nu_{\text{PS}}) + \alpha_{\text{PS}}\Delta T \quad (1)$$

$$\epsilon_z = -\frac{2\nu_{\text{PS}}}{E_{\text{PS}}}\sigma + \alpha_{\text{PS}}\Delta T \quad (2)$$

where we define E_{PS} , ν_{PS} , and α_{PS} as the modulus, Poisson's ratio, and linear thermal expansion coefficient of PS. The PS strain is forced to match the thermal expansion of the underlying support (e.g., silicon), in the x and y directions

$$\epsilon_x = \epsilon_y = \alpha_{\text{sup}}\Delta T \quad (3)$$

such that eqs 1 and 3 can be used to solve for the equibiaxial in-plane stress imparted to the PS:

$$\sigma = \frac{-E_{\text{PS}}}{1 - \nu_{\text{PS}}}[\alpha_{\text{PS}} - \alpha_{\text{sup}}]\Delta T \quad (4)$$

The negative sign out front in eq 4 means that on cooling (negative ΔT) a positive stress is generated implying tension in the film, as the thermal expansion coefficient of PS is larger than that of the rigid support for all frame materials studied here. (Note that in other works this negative sign may be omitted^{31,32} or ΔT defined differently.⁸ In eq 9, the limits of integration have been swapped to accommodate the negative sign.)

The PS strain in the z direction will be affected by this equibiaxial stress, which, by substituting eq 4 into eq 2, is

$$\epsilon_z = \alpha_{\text{PS}}\Delta T + \frac{2\nu_{\text{PS}}}{1 - \nu_{\text{PS}}}[\alpha_{\text{PS}} - \alpha_{\text{sup}}]\Delta T \quad (5)$$

such that on cooling, negative ΔT , both terms lead to a decrease in ϵ_z , i.e., film contraction. Equation 5 is useful because the measured thermal expansion coefficient determined from the film thickness h by ellipsometry is

$$\alpha_{\text{measured}} = \frac{1}{h} \left(\frac{dh}{dT} \right) = \frac{\epsilon_z}{\Delta T} \quad (6)$$

such that from eq 5, we get

$$\alpha_{\text{measured}} = \alpha_{\text{PS}} + \frac{2\nu_{\text{PS}}}{1 - \nu_{\text{PS}}}[\alpha_{\text{PS}} - \alpha_{\text{sup}}] \quad (7)$$

Thus, eq 7 demonstrates that the experimentally measured thermal expansion coefficient, α_{measured} , typically determined from the temperature dependence of the film thickness $h(T)$, is not the same as the stress-free, “true” linear thermal expansion coefficient of PS, α_{PS} , but is altered by the thermal expansion coefficient of the underlying support, α_{sup} , and the Poisson's ratio of PS, ν_{PS} . However, eq 7 also enables us to determine the “true” (or corrected) linear thermal expansion coefficient of PS from standard film thickness measurements:

$$\alpha_{\text{PS}} = \left(\frac{1 - \nu_{\text{PS}}}{1 + \nu_{\text{PS}}} \right) \alpha_{\text{measured}} + \left(\frac{2\nu_{\text{PS}}}{1 + \nu_{\text{PS}}} \right) \alpha_{\text{sup}} \quad (8)$$

If we consider typical values for α_{measured} above and below T_g , we get good agreement with literature values for the “true” (corrected) linear thermal expansion coefficient for PS quoted in polymer handbooks.³⁹ In the glassy region below T_g , $\nu_{\text{PS}} \approx 1/3$, such that $\alpha_{\text{PS}} \approx 1/2\alpha_{\text{measured}} + 1/2\alpha_{\text{sup}}$, while in the melt region above T_g , $\nu_{\text{PS}} \approx 1/2$, such that $\alpha_{\text{PS}} \approx 1/3\alpha_{\text{measured}} + 2/3\alpha_{\text{sup}}$. For PS on silicon ($\alpha_{\text{sup}} \approx 3 \times 10^{-6} \text{ K}^{-1}$), ellipsometry measurements typically give $\alpha_{\text{measured}} \approx 1.6 \times 10^{-4} \text{ K}^{-1}$ below T_g and $\alpha_{\text{measured}} \approx 6 \times 10^{-4} \text{ K}^{-1}$ above T_g ^{40–43} which correspond to “true”, corrected linear thermal expansion coefficients for PS of $\alpha_{\text{PS}} \approx 0.8 \times 10^{-4} \text{ K}^{-1}$ in the glassy region below T_g and $\alpha_{\text{PS}} \approx 2 \times 10^{-4} \text{ K}^{-1}$ in the melt region above T_g , in agreement with values found in polymer handbooks³⁹ and bulk dilatometry⁴⁴ (with $\alpha_{\text{volume}} = 3\alpha_{\text{linear}}$ in the stress-free state typically experienced in dilatometry).

Returning now to the calculation of the equibiaxial in-plane stress imparted to the PS film, because E_{PS} , ν_{PS} , and α_{PS} are all strong functions of temperature, changing dramatically through T_g , eq 4 needs to be solved in integral form:

$$\sigma(T_g, T_{\text{aging}}) = \int_{T_{\text{aging}}}^{T_g} \frac{E_{\text{PS}}(T)}{1 - \nu_{\text{PS}}(T)} [\alpha_{\text{PS}}(T) - \alpha_{\text{sup}}(T)] dT \quad (9)$$

with the stress depending on the temperature range over which the film is cooled. Equation 9, representing the initial stress imparted to the films after cooling, has been found to agree well with experimental measures of the stress formed on cooling for PS films supported on substrates.^{31,32} Thus, even though eq 9 treats the polymer film as a purely elastic material, this turns out to be a remarkably good approximation, suggesting that a formal viscoelastic treatment would only result in a small correction. As discussed and verified previously by Gray et al.,⁸ stress does not begin to build up in the PS film as long as it remains an equilibrium liquid above T_g , as experimentally found by Zhao et al.³¹ from direct measurements of the stress. Consequently, regardless of the initial annealing temperature above T_g , the relevant temperature range for eq 9 is from T_g down to the aging temperature T_{aging} . Note that the stress builds up slowly upon cooling below T_g , such that even for the case of PS on silicon (the largest stress values in the present study), the stress from thermal expansion mismatch is still well below the yield stress of the material.

Both supported films and free-standing films held by a rigid frame across a circular opening experience the same in-plane equibiaxial stress, given by eq 9, imparted during the thermal quench due to the mismatch in thermal expansion between the film and support. From eq 9, it is clear that the stress imparted

to the films on cooling depends directly on the difference in thermal expansion coefficient between the PS film and rigid support over the temperature range cooled. Thus, to determine the stress imparted to the films on cooling, we first need temperature-dependent values for the linear thermal expansion coefficient of the materials of interest.

The “true”, corrected linear thermal expansion coefficients of the polymers studied here (PS, PSF, and PC) were determined via eq 8 from ellipsometry measurements of the temperature-dependent film thickness $h(T)$ for bulk (~ 500 nm thick) films on silicon measured at $1^\circ\text{C}/\text{min}$ on cooling, where α_{measured} was calculated using eq 6. Tabulated values for the temperature-dependent linear thermal expansion coefficients of silicon⁴⁵ and Poisson’s ratio of PS⁴⁶ were used, while the Poisson’s ratios of PSF and PC were taken to be $\nu_{\text{PSF}} = 0.37$ and $\nu_{\text{PC}} = 0.38$ based on manufacturers’ specifications across the temperature range of T_g^{PS} to T_{aging} where PSF and PC remain in their glassy state. Figure 4a plots the temperature dependence of the measured thermal expansion coefficient α_{measured} for a 500 nm thick PS film on silicon, determined via eq 6, and the corrected (“true”) linear thermal expansion coefficient of PS, α_{PS} , determined using eq 8. From the graph in Figure 4a, we can see that the largest difference between the measured and “true” thermal expansion coefficients occur above T_g in the melt state. This arises because Poisson’s ratio for PS is larger in the melt state, as a nearly incompressible liquid. From eq 7, a larger fraction of the underlying silicon’s thermal expansion will contribute when ν_{PS} is larger. To compare the various materials used in the present study, Figure 4b plots the temperature dependence of the true (corrected) linear thermal expansion coefficient of PS, PSF, PC, silicon,⁴⁵ (304) stainless steel,⁴⁷ and (6061) aluminum,⁴⁸ where tabulated literature values have been used for the various inorganic materials.

The temperature-dependent linear thermal expansion coefficients presented in Figure 4b enable direct comparison of the thermal expansion mismatch between PS and the various materials for the supporting frames. The magnitude of the relative stress differences between the various materials will depend directly on the integrated thermal expansion mismatch over the temperature range that stress builds up in the PS films: $T_g^{\text{PS}} = 100^\circ\text{C}$ to $T_{\text{aging}} = 65^\circ\text{C}$. For easy comparison, we list in Table 1 the thermal expansion coefficient (average value over the temperature range of 65 – 100°C , although the values vary by less than 8% over this range) and the integrated thermal expansion mismatch with PS for the various supporting frame materials used in the present study. This thermal expansion mismatch $\Delta\alpha$ was calculated numerically, from $T_g^{\text{PS}} = 100^\circ\text{C}$ to $T_{\text{aging}} = 65^\circ\text{C}$, as

$$\Delta\alpha = \int_{T_{\text{aging}}}^{T_g} [\alpha_{\text{PS}}(T) - \alpha_{\text{sup}}(T)] dT \quad (10)$$

using the data presented in Figure 4b. Formally, this is equivalent to the total strain built up in the glassy PS film as it is cooled below its T_g . These $\Delta\alpha$ values are a robust measure of the relative magnitude of the stress differences imparted by the various frame materials and are perhaps more reliable than the explicit values of stress calculated from eq 9 because they do not depend on the Young’s modulus of PS, $E_{\text{PS}}(T)$. Although the temperature-dependent Poisson’s ratio for PS changes only from 0.5 to 0.35 in going from the melt to the glassy state, Young’s modulus $E_{\text{PS}}(T)$ varies by more than 3 orders of magnitude.

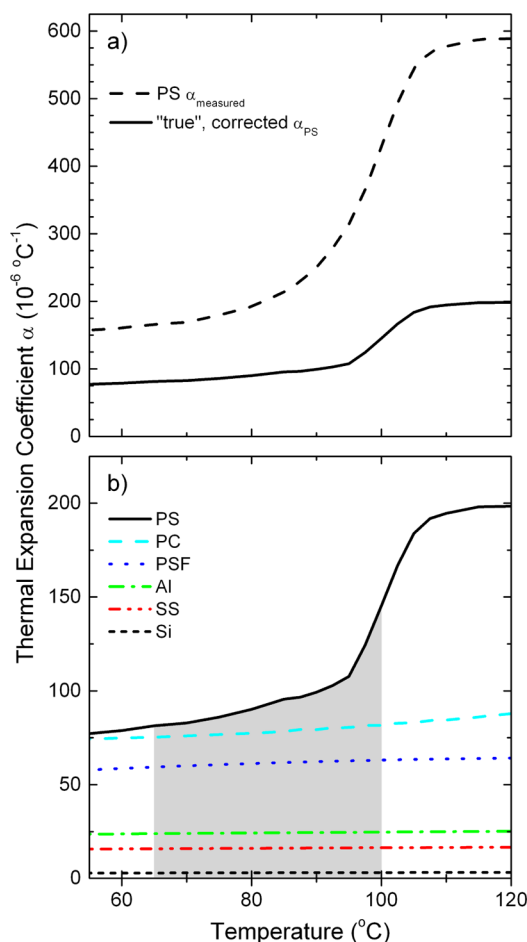


Figure 4. Temperature-dependent thermal expansion coefficients, $\alpha(T)$: (a) PS α_{measured} based on film thickness $h(T)$ data using eq 6, measured on cooling at $1^\circ\text{C}/\text{min}$ for a 500 nm thick PS film supported on Si using ellipsometry (dashed line). The “true” α_{PS} , corrected using eq 8 to remove the vertical strain component induced by the underlying silicon, is plotted as a solid curve. (b) “True” α for all of the materials used in this study where the relevant temperature range for stress buildup on cooling ($T_g^{\text{PS}} = 100^\circ\text{C}$ to $T_{\text{aging}} = 65^\circ\text{C}$) has been highlighted. “True” α for the polymers [PS (solid black line), PSF (dashed cyan line), PC (dotted blue line)] is corrected using eq 8 from measurements on cooling at $1^\circ\text{C}/\text{min}$ for bulk (~ 500 nm) films supported on Si. Tabulated data are used for Al (dash-dot green line),⁴⁸ SS (dash-dot-dot red line),⁴⁷ and Si (short dashed black line).⁴⁵

Table 1. Thermal Expansion Coefficient α , Integrated Thermal Expansion Mismatch $\Delta\alpha$ Relative to PS from Eq 10, Stress σ Imparted to the PS Films on cooling to $T_{\text{aging}} = 65^\circ\text{C}$ Based on Eq 9 for the Various Materials Used in the Present Study, and Physical Aging Rate β_{PS} (Average of 3–5 Measurements) for ~ 500 nm Thick Free-Standing PS Films Held by Frames of the Materials Listed (or Supported on Silicon) at 65°C

frame material	α ($10^{-6}^\circ\text{C}^{-1}$)	$\Delta\alpha$ with PS	σ (MPa)	β_{PS} (10^{-4})
PC	78.1	0.000 64	0.7	4.8 ± 0.2
PSF	61.4	0.001 23	1.7	6.5 ± 0.6
Al	23.8	0.002 54	4.0	6.6 ± 0.5
SS	16.1	0.002 81	4.5	8.7 ± 0.4
Si	2.97	0.003 27	5.3	8.9 ± 0.4
supported on Si	2.97	0.003 27	5.3	9.2 ± 0.5

To explicitly calculate the stress imparted to the films via eq 9, values for the temperature-dependent Young's modulus of PS, $E_{\text{PS}}(T)$, are also needed. The precise values of the stress imparted to the films depend significantly on the values of $E_{\text{PS}}(T)$ because $E_{\text{PS}}(T)$ changes by more than 3 orders of magnitude over the temperature range that the stress builds up on cooling. Obtaining reliable values for the temperature-dependent Young's modulus of PS from the literature proved to be harder than expected, such that future measurements of $E_{\text{PS}}(T)$ on even bulk PS films would be warranted. For the present calculation, we decided to use the $E_{\text{PS}}(T)$ data given in Beaucage et al.⁴⁶ because they are matched with reasonable $\nu_{\text{PS}}(T)$ data, a rare occurrence,⁴⁹ and the stress values calculated from eq 9 using these data for PS films supported on silicon cooled to room temperature ($\sigma \approx 15$ MPa) were found to be consistent with independent experimental measures of the stress (15–16 MPa) for such samples.^{31,32} Values of the equibiaxial in-plane stress imparted to PS films, upon cooling to an aging temperature of 65 °C, when supported by rigid frames of the various materials studied are included in Table 1 based on numerical integration of eq 9. We note that even though the $E_{\text{PS}}(T)$ data may not be the most ideal, we are confident in the values of thermal expansion coefficients that define the thermal expansion mismatch between the different materials. Because $E_{\text{PS}}(T)$ only shows up as a numerical prefactor in eq 9 and the $\alpha(T)$ data for the frame materials all have similarly weak temperature dependences, we are confident in the relative differences between the different stress values calculated, which is what is found to correlate with the relative differences in physical aging rate.

Correlating Physical Aging Rate with Thermal Expansion Mismatch and Applied Stress. The expression for the equibiaxial in-plane stress σ , given by eq 9, imparted during the thermal quench (i.e., glass formation) due to the thermal expansion mismatch between film and support explicitly shows that there is no film thickness dependence to the stress for free-standing films supported on rigid (non-flexible) frames or for supported films on rigid substrates. Thus, the results presented in Figure 3 showing no change in physical aging rate with film thickness for free-standing PS films (220–1800 nm thick) held by SS frames are in agreement with films of all thicknesses being formed with the same stress value. In addition, the results represented in Figure 2 are consistent with the idea that the physical aging rate is affected by stress imparted during the thermal quench with larger stresses leading to larger aging rates because the stress for PS films supported on silicon ($\sigma \approx 5.3$ MPa) is slightly larger than that for free-standing PS films held by rigid SS frames ($\sigma \approx 4.5$ MPa), as shown in Table 1.

To further test the idea that stress resulting from thermal expansion mismatch between film and support correlates with the observed physical aging rates, we have made rigid frames containing a circular opening from materials with different thermal expansion coefficients. For example, PSF and PC have thermal expansion coefficients significantly different from SS and Si and much closer to PS (see Table 1). Figure 5 compares the observed physical aging at 65 °C for ~500 nm thick free-standing PS films held by PC, PSF, SS, and Si as well as a 482 nm thick PS film supported on Si. We find that the observed physical aging rates correlate with the stress imparted to the films due to the thermal expansion mismatch between film and support, as given by eq 9. The average physical aging rates (based on 3–5 measurements) for ~500 nm thick PS films are

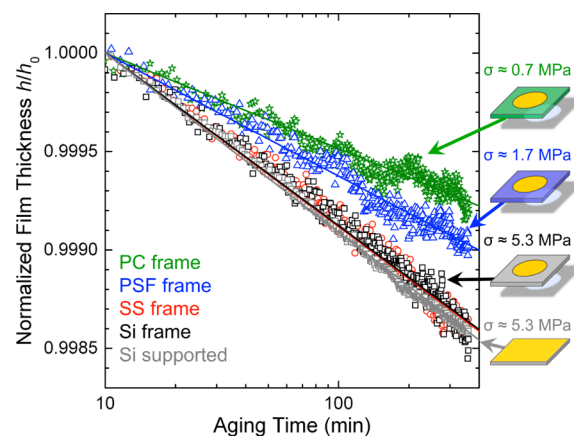


Figure 5. Normalized film thickness h/h_0 vs logarithmic aging time for ~500 nm thick PS films held free-standing on a PC frame (green stars), PSF frame (blue triangles), SS frame (red circles), and silicon frame (black squares) as well as for a supported PS film on silicon (gray squares). Physical aging rates (average of 3–5 samples) correlate with the stress imparted on cooling from thermal expansion mismatch between film and support as listed in Table 1.

listed in Table 1. The lowest physical aging rate, $\beta = (4.8 \pm 0.2) \times 10^{-4}$, is observed for free-standing films held by PC frames that impart the lowest stress, $\sigma \approx 0.7$ MPa, while the highest aging rates are $\beta = (8.9 \pm 0.4) \times 10^{-4}$ for free-standing films on silicon frames and $\beta = (9.2 \pm 0.5) \times 10^{-4}$ for supported films on silicon, both with $\sigma \approx 5.3$ MPa, the highest stress. The data are consistent with eq 9 predicting that both free-standing and supported films have the same stress ($\sigma \approx 5.3$ MPa) for the same supporting material.

Figure 6 demonstrates the correlation between the observed physical aging rate at 65 °C for ~500 nm thick PS films with the thermal expansion mismatch $\Delta\alpha$ and applied stress σ . Data shown are based on measurements collected on 3–5 nominally identical samples of free-standing PS films for each of the different frame materials: Si, SS, Al, PSF, and PC (open red circles). A data point (solid back square) is also included for PS films supported on silicon wafers. The same physical aging rate is observed for free-standing and supported films when held by frames (or substrates) of the same material, consistent with the stress prediction from eq 9 where the equibiaxial in-plane stress depends only on the thermal expansion mismatch between film and support. We plot the physical aging rate both as a function of thermal expansion mismatch $\Delta\alpha$ and stress σ because $\Delta\alpha$ is the more well-defined quantity. As discussed above, the absolute value of stress strongly depends on the $E(T)$ literature data used for PS, as it varies by more than 3 orders of magnitude over the temperature range integrated in eq 9. However, note that the relative differences in the stress between the various frame materials are reliable because they depend only on the relative difference in thermal expansion coefficients. It is clear from the data that a larger thermal expansion mismatch $\Delta\alpha$, and hence stress σ buildup on cooling, results in a larger physical aging rate, where the increased stress from $\sigma_{\text{PC}} \approx 0.7$ MPa to $\sigma_{\text{Si}} \approx 5.3$ MPa leads to a near doubling of the physical aging rate of ~500 nm thick free-standing PS films aged at 65 °C. There is no reason to believe that the trend in $\beta(\sigma)$ should be linear, and future work will focus on measuring $\beta(\sigma)$ by directly controlling stress on cooling.

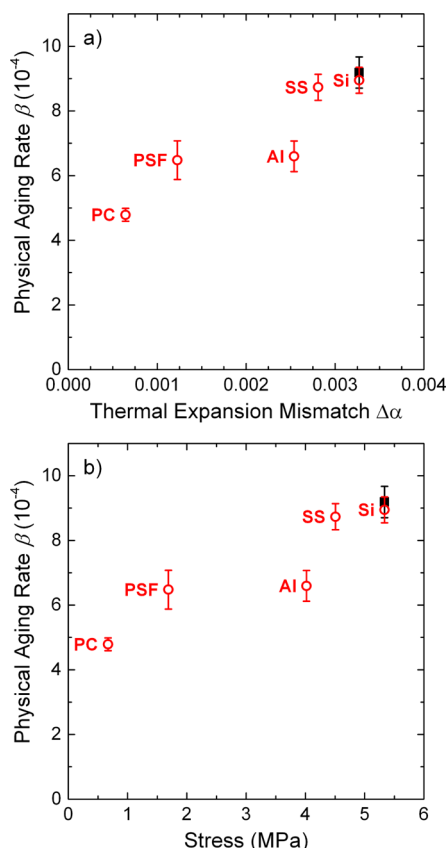


Figure 6. Physical aging rate β for ~500 nm thick PS films aged at 65 °C as a function of (a) thermal expansion mismatch $\Delta\alpha$ between PS and the supporting frame material, as defined in eq 10, and (b) stress imparted to PS on cooling to 65 °C as determined by eq 9 for the different supporting frame materials: polycarbonate (PC), polysulfone (PSF), aluminum (Al), stainless steel (SS), and silicon (Si). Data plotted are based on an average of 3–5 samples with free-standing PS films held by rigid frames containing circular openings shown as open red circles, while that for supported PS films on Si is given as a solid black square.

DISCUSSION

Given this correlation between stress and physical aging, we reconsider in this context previous reports in the literature that made efforts to correlate physical aging with sample-size dependence. Often cited as the first such test, Braun and Kovacs compared the physical aging behavior of powdered PS samples (containing fibrous sheets 100–1000 nm in thickness) with bulk (same powdered PS molded into 1 mm thick samples).⁵⁰ They found that the physical aging rate of PS did not depend on the sample geometry or “state of division of the sample”. This study would be in agreement with the present work as the powdered and molded samples suspended in a mercury filled dilatometer would be unconstrained and free to thermally expand and contract as necessary.

Recently, Gray et al.⁸ found that thickness-dependent faster physical aging for micrometer thick PS films only occurred when samples were supported on a wire frame during the thermal quench. In this study, the free-standing PS films were supported by 0.009 in. diameter stainless spring steel wire frames with the PS film spanning across two sides of the rectangular wire frame during the annealing step and thermal quench from above T_g down to room temperature before being transferred onto silicon wafers for the aging measurements. The

aging rate at 65 °C for PS free-standing films held by these wire frames during the thermal quench were $\beta = (6.1 \pm 0.6) \times 10^{-4}$ for 1380 \pm 100 nm thick films and $\beta = (8.1 \pm 0.6) \times 10^{-4}$ for 570 \pm 50 nm thick films. In contrast, when these same thickness films were quenched supported on silicon ($\sigma = 5.3$ MPa according to Table 1), the aging rates were $\beta = (9.5 \pm 0.6)$ and $\beta = (9.3 \pm 0.6)$.⁸ Because Gray et al. observed that film-thickness-dependent physical aging only occurred when samples were supported on these wire frames during the thermal quench, they hypothesized that the wire frames acted as small springs imparting a force F leading to a film-thickness-dependent stress $\sigma = F/(hw)$ applied to the films during the quench, where (hw) represents the cross-sectional area (height \times width) of the films.⁸ Efforts to directly quantify this stress were not possible. Although Gray et al. proposed and attempted physical aging measurements of free-standing films quenched on rigid frames that would impart thickness-independent stresses, such measurements were not successful until the improvements made here in the present study. From the β vs stress data presented in Figure 6b, we can extrapolate that the physical aging rate for PS films quenched stress free should be $\sim 4 \times 10^{-4}$. Thus, it would appear from the aging rates measured for the PS films held by the wire frames that the stresses imparted to these films are quite substantial. A direct comparison cannot be made because the sample geometry in the present study imparts a biaxial stress compared with the uniaxial stress imparted by the rectangular wire frames. However, separate measurements in our lab applying uniaxial stresses find a similar β vs stress behavior and the same aging rate of $\sim 4 \times 10^{-4}$ in the limit of zero stress. As PS has been shown to not be a good model system⁵¹ for gas separation membranes, these conclusions of how stress imparted during the thermal quench can affect the subsequent physical aging rate would need to be tested on the higher T_g , stiff backbone polymers that are used as gas separation membranes (e.g., PSF, polyimide, etc.), in particular at the operating temperatures used for gas separation (typically 35 °C), before any broad applicability could be made.

Simon et al. have also correlated changes in physical aging upon confinement with increased stress (hydrostatic tension) resulting from thermal expansion mismatch between the glass former (*o*-terphenyl) and surrounding support (nanoporous matrix).³⁴ However, in this study it is the time to reach equilibrium that was accelerated, with insufficient data presented to comment on the aging rate itself. Unfortunately, a number of studies have involved sample geometries for which it is not possible to estimate what unintended stresses might be imparted during thermal cooling.^{10,24,29,30,52–54} In several such studies, it is not the aging rate that is faster, but the time to reach equilibrium that is “accelerated”.^{10,29,30,53,54} Work by Priestley et al. on silica-capped PS nanospheres may enable further confirmation of how stress development from thermal expansion mismatch during thermal cooling affects physical aging by being able to more finely control internal stresses.^{35,55}

For this discussion we omit the numerous studies that have observed changes in physical aging rate at length scales \sim 100 nm or less,^{11–18} some of which have been directly correlated with T_g changes.^{11–14,16,18} Such “nanoconfinement” effects *do* correlate with the surface-to-volume ratio of samples such that free volume diffusion type models^{56,57} may be effective in explaining glassy dynamics at these smaller length scales.

The nature of how deformation (stress or strain) imparts mobility to glasses is a long-standing problem that unifies

concepts in polymer glasses, colloids, and granular materials.⁵⁸ In theoretical models, stress or strain is treated as facilitating energy barrier hopping^{59,60} or equivalently tilting of the potential energy landscape,^{61,62} an idea that was originally proposed by Eyring.⁶³ Such an interpretation of stress-induced mobility in polymer glasses is supported by work that shows glassy dynamics not correlating with free volume,^{64–66} but depending on a glass' position within the energy landscape.^{62,67} The vast majority of studies in this field on how mobility is increased by the application of mechanical stress or strain investigate glasses that have been formed stress free. The present work is different in that the stress is applied during glass formation (vitrification) and that even the presence of small stresses is found to have a noticeable effect on the subsequent physical aging and stability of the material. Future studies of how physical aging in polymer glasses can be altered by stress during glass formation by directly controlling the stress on cooling are underway.

CONCLUSIONS

The results presented here demonstrate that there is no thickness dependence to the physical aging rate for free-standing PS films, for thicknesses between 220 and 1800 nm, when held by rigid frames that impart a thickness-independent stress on cooling. This is consistent with data for supported films on silicon, which also have a constant, thickness-independent stress imparted to them on cooling, that show the physical aging rate is independent of film thickness above ~100 nm^{8,11} (i.e., where T_g is equivalent to bulk). These combined results for free-standing and supported films held by rigid supports observe no inherent film thickness dependence to physical aging (for films >200 nm in thickness). Our conclusion is that the physical aging rate of free-standing PS films correlates with the stress imparted to the films during cooling (i.e., glass formation) due to thermal expansion mismatch between film and support.

AUTHOR INFORMATION

Corresponding Author

*E-mail: cbroth@emory.edu (C.B.R.).

Notes

The authors declare no competing financial interest.

ACKNOWLEDGMENTS

We thank Laura A. G. Gray for useful discussions and acknowledge financial support from Emory University.

REFERENCES

- Priestley, R. D. *Soft Matter* **2009**, *5*, 919–926.
- Huang, Y.; Paul, D. R. *Ind. Eng. Chem. Res.* **2007**, *46*, 2342–2347.
- Pfromm, P. H.; Koros, W. J. *Polymer* **1995**, *36*, 2379–2387.
- Dorkenoo, K. D.; Pfromm, P. H. *Macromolecules* **2000**, *33*, 3747–3751.
- McCaig, M. S.; Paul, D. R. *Polymer* **2000**, *41*, 629–637.
- Huang, Y.; Paul, D. R. *Polymer* **2004**, *45*, 8377–8393.
- Huang, Y.; Paul, D. R. *J. Membr. Sci.* **2004**, *244*, 167–178.
- Gray, L. A. G.; Yoon, S. W.; Pahner, W. A.; Davidheiser, J. E.; Roth, C. B. *Macromolecules* **2012**, *45*, 1701–1709.
- Huang, Y.; Paul, D. R. *Macromolecules* **2006**, *39*, 1554–1559.
- Boucher, V. M.; Cangialosi, D.; Alegria, A.; Colmenero, J. *Macromolecules* **2012**, *45*, 5296–5306.
- Pye, J. E.; Rohald, K. A.; Baker, E. A.; Roth, C. B. *Macromolecules* **2010**, *43*, 8296–8303.
- Kawana, S.; Jones, R. A. L. *Eur. Phys. J. E* **2003**, *10*, 223–230.
- Priestley, R. D.; Broadbelt, L. J.; Torkelson, J. M. *Macromolecules* **2005**, *38*, 654–657.
- Priestley, R. D.; Ellison, C. J.; Broadbelt, L. J.; Torkelson, J. M. *Science* **2005**, *309*, 456–459.
- Fukao, K.; Sakamoto, A. *Phys. Rev. E* **2005**, *71*, 041803.
- Koh, Y. P.; Simon, S. L. *J. Polym. Sci., Part B: Polym. Phys.* **2008**, *46*, 2741–2753.
- Rowe, B. W.; Freeman, B. D.; Paul, D. R. *Polymer* **2009**, *50*, 5565–5575.
- Frieberg, B.; Glynos, E.; Green, P. F. *Phys. Rev. Lett.* **2012**, *108*, 268304.
- Roth, C. B.; Dutcher, J. R. *J. Electroanal. Chem.* **2005**, *584*, 13–22.
- Pye, J. E.; Roth, C. B. *Phys. Rev. Lett.* **2011**, *107*, 235701.
- McCaig, M. S.; Paul, D. R.; Barlow, J. W. *Polymer* **2000**, *41*, 639–648.
- Thornton, A. W.; Hill, A. J. *Ind. Eng. Chem. Res.* **2010**, *49*, 12119–12124.
- Huang, Y.; Wang, X.; Paul, D. R. *J. Membr. Sci.* **2006**, *277*, 219–229.
- Cangialosi, D.; Wubbenhorst, M.; Groenewold, J.; Mendes, E.; Schut, H.; van Veen, A.; Picken, S. J. *Phys. Rev. B* **2004**, *70*, 224213.
- Curro, J. G.; Lagasse, R. R.; Simha, R. *Macromolecules* **1982**, *15*, 1621–1626.
- Alfrey, T.; Goldfinger, G.; Mark, H. J. *Appl. Phys.* **1943**, *14*, 700–705.
- Rowe, B. W.; Pas, S. J.; Hill, A. J.; Suzuki, R.; Freeman, B. D.; Paul, D. R. *Polymer* **2009**, *50*, 6149–6156.
- Huang, Y.; Paul, D. R. *J. Polym. Sci., Part B: Polym. Phys.* **2007**, *45*, 1390–1398.
- Boucher, V. M.; Cangialosi, D.; Alegria, A.; Colmenero, J.; Gonzalez-Irun, J.; Liz-Marzan, L. M. *Soft Matter* **2010**, *6*, 3306–3317.
- Cangialosi, D.; Boucher, V. M.; Alegria, A.; Colmenero, J. *J. Chem. Phys.* **2011**, *135*, 014901.
- Zhao, J. H.; Kiene, M.; Hu, C.; Ho, P. S. *Appl. Phys. Lett.* **2000**, *77*, 2843–2845.
- Chung, J. Y.; Chastek, T. Q.; Fasolka, M. J.; Ro, H. W.; Stafford, C. M. *ACS Nano* **2009**, *3*, 844–852.
- Thomas, K. R.; Steiner, U. *Soft Matter* **2011**, *7*, 7839–7842.
- Simon, S. L.; Park, J. Y.; McKenna, G. B. *Eur. Phys. J. E* **2002**, *8*, 209–216.
- Guo, Y.; Zhang, C.; Lai, C.; Priestley, R. D.; D'Acunzi, M.; Fytas, G. *ACS Nano* **2011**, *5*, 5365–5373.
- Baker, E. A.; Rittigstein, P.; Torkelson, J. M.; Roth, C. B. *J. Polym. Sci., Part B: Polym. Phys.* **2009**, *47*, 2509–2519.
- Struik, L. C. E. *Physical Aging in Amorphous Polymers and Other Materials*; Elsevier Scientific Publishing Company: Amsterdam, 1978.
- Benham, P. P.; Crawford, R. J.; Armstrong, C. G. *Mechanics of Engineering Materials*, 2nd ed.; Addison Wesley Longman: London, 1996.
- Polymer Handbook*, 4th ed.; Brandrup, J.; Immergut, E. H., Grulke, E. A., Abe, A., Bloch, D. H., Eds.; Wiley: New York, 1999.
- Kawana, S.; Jones, R. A. L. *Phys. Rev. E* **2001**, *63*, 021501.
- Seemann, R.; Jacobs, K.; Landfester, K.; Herminghaus, S. *J. Polym. Sci., Part B: Polym. Phys.* **2006**, *44*, 2968–2979.
- Kim, S.; Hewlett, S. A.; Roth, C. B.; Torkelson, J. M. *Eur. Phys. J. E* **2009**, *30*, 83–92.
- Miyazaki, T.; Nishida, K.; Kanaya, T. *Phys. Rev. E* **2004**, *69*, 061803.
- Simon, S. L.; Sobieski, J. W.; Plazek, D. J. *Polymer* **2001**, *42*, 2555–2567.
- Okada, Y.; Tokumaru, Y. *J. Appl. Phys.* **1984**, *56*, 314–320.
- Beaucage, G.; Composto, R.; Stein, R. S. *J. Polym. Sci., Part B: Polym. Phys.* **1993**, *31*, 319–326.
- Bogaard, R. H.; Desai, P. D.; Li, H. H.; Ho, C. Y. *Thermochim. Acta* **1993**, *218*, 373–393.
- Metallic Materials Properties Development and Standardization (MMPDS-05) Handbook*; Battelle Memorial Institute: Columbus, OH, 2013; pp 3–370.

- (49) Tschoegl, N. W.; Knauss, W. G.; Emri, I. *Mech. Time-Depend. Mater.* **2002**, *6*, 3–51.
- (50) Braun, G.; Kovacs, A. J. *Phys. Chem. Glasses* **1963**, *4*, 152–160.
- (51) Murphy, T. M.; Freeman, B. D.; Paul, D. R. *Polymer* **2013**, *54*, 873–880.
- (52) Cangialosi, D.; Wubbenhorst, M.; Groenewold, J.; Mendes, E.; Picken, S. J. *J. Non-Cryst. Solids* **2005**, *351*, 2605–2610.
- (53) Boucher, V. M.; Cangialosi, D.; Alegria, A.; Colmenero, J. *Macromolecules* **2010**, *43*, 7594–7603.
- (54) Boucher, V. M.; Cangialosi, D.; Alegria, A.; Colmenero, J.; Pastoriza-Santos, I.; Liz-Marzan, L. M. *Soft Matter* **2011**, *7*, 3607–3620.
- (55) Zhang, C.; Guo, Y.; Priestley, R. D. *J. Polym. Sci., Part B: Polym. Phys.* **2013**, *51*, 574–586.
- (56) Tito, N. B.; Lipson, J. E. G.; Milner, S. T. *Soft Matter* **2013**, *9*, 3173–3180.
- (57) Tito, N. B.; Lipson, J. E. G.; Milner, S. T. *Soft Matter* **2013**, *9*, 9403–9413.
- (58) Roth, C. B. *J. Polym. Sci., Part B: Polym. Phys.* **2010**, *48*, 2558–2560.
- (59) Chen, K.; Schweizer, K. S. *Europhys. Lett.* **2007**, *79*, 26006.
- (60) Chen, K.; Schweizer, K. S. *Macromolecules* **2011**, *44*, 3988–4000.
- (61) Lacks, D. J.; Osborne, M. J. *Phys. Rev. Lett.* **2004**, *93*, 255501.
- (62) Chung, Y. G.; Lacks, D. J. *J. Phys. Chem. B* **2012**, *116*, 14201–14205.
- (63) Eyring, H. *J. Chem. Phys.* **1936**, *4*, 283–291.
- (64) Riggleman, R. A.; Lee, H.-N.; Ediger, M. D.; de Pablo, J. J. *Phys. Rev. Lett.* **2007**, *99*, 215501.
- (65) Colucci, D. M.; O'Connell, P. A.; McKenna, G. B. *Polym. Eng. Sci.* **1997**, *37*, 1469–1474.
- (66) Smith, T. L.; Levita, G.; Moonan, W. K. *J. Polym. Sci., Part B: Polym. Phys.* **1988**, *26*, 875–881.
- (67) Riggleman, R. A.; Schweizer, K. S.; de Pablo, J. J. *Macromolecules* **2008**, *41*, 4969–4977.